INFLUENCE OF THE BLOWOFF OF BOUNDARY GAS FROM THE DISCHARGE CHAMBER OF A PLASMATRON ON THE PARAMETERS OF THE JET

J. Dundr, F. Plojhar,
and J. Slechta

UDC 533.9.07

The results of an experimental investigation of the parameters of an argon jet heated in a plasmatron with an anode permitting the removal of part of the cool gas from the discharge chamber are presented.

1. Introduction

Highly heated, partially ionized gases are presently used in various technological processes (e.g., [1-3]). In this connection, considerable interest is paid to the study of the parameters of gas jets heated in plasmatrons of various constructions. Some results of research on the hydrodynamic structure of the gas stream carried out at the Institute of Thermomechanics, Academy of Sciences of Czechoslovakia, are given in [4-6].

Variation of the parameters of the gas jet, the degree of heating of which depends on the plasmatron construction, is achieved most often by varying either the parameters of the power-supply circuit or the amount of the working gas. The possibilities of hydrodynamic action through the injection of cool gas directly into the escaping stream behind the anode or into the discharge chamber ahead of the anode are used considerably less often [7]. In plasmatrons with vortex stabilization of the electric arc and with a converging nozzle one can also use the fact that a considerable part of the gas flows through the discharge chamber outside the region of the electric arc. In this case the mixing of gases occurs in the anode nozzle [8]. Using a special construction of the anode unit, part of the cool gas can be removed from the discharge chamber of the plasmatron through a slit [9, 10].

Let us proceed to give the results of an investigation of the parameters of a free argon jet escaping from an anode unit. In the experiment we measured the maximum velocity and maximum temperature of the heated argon jet near the nozzle cut for different values of the width of the slit between the anode and the discharge chamber. On the basis of the measured temperatures we also obtained information about the transverse size of the radiating core of the jet.

2. Experimental Setup and Measuring Diagnostics

A plasmatron described in [5, 8] was used in the tests. A diagram of the plasmatron with the proposed construction of the anode unit is shown in Fig. 1. The active part 1 of the cathode is built of tungsten with an admixture of thorium. The auxiliary cathode and anode (for initiating the electric arc with a high-frequency voltage), designated as − and + in Fig. 1, are separated by an interlayer 2 of textolite. The argon enters tangentially into the entrance vortex chamber through an opening in the interlayer 2 mm in diameter. The discharge chamber 3 with a diameter of 15 mm consists of three electically insulated parts cooled by water. To make measurements inside the discharge chamber there are four probe openings in each part of it, placed opposite to one another. The anode unit contains an electrically passive intermediate element 4 and the anode proper 5 with a diameter of 8 mm.

To prevent movement of the anode spot, a layer of heat-resistant dielectric material is deposited by plasma sputtering on the lower surface of the anode in the region of the slit. The main anode is fastened to the support with a holder 6 and can be moved in the direction of the plasmatron axis. In this way a slit 7 with the required width s can be created with an accuracy of ±0.02 mm. In our experiments the slit width was varied from 0.5 to 2 mm. Measurements with s = 0 were not made, since the thickness of plasma sputtering of the insulation layer was nonuniform, and so leakage of argon occurred.

Institute of Thermomechanics, Academy of Sciences of Czechoslovakia, Prague. Translated from Inzhenerno-Fizicheskii Zhurnal, Vol. 52, No. 1, pp. 141-148, January, 1987. Original article submitted December 26, 1985.

0022-0841/87/5201-0115$12.50

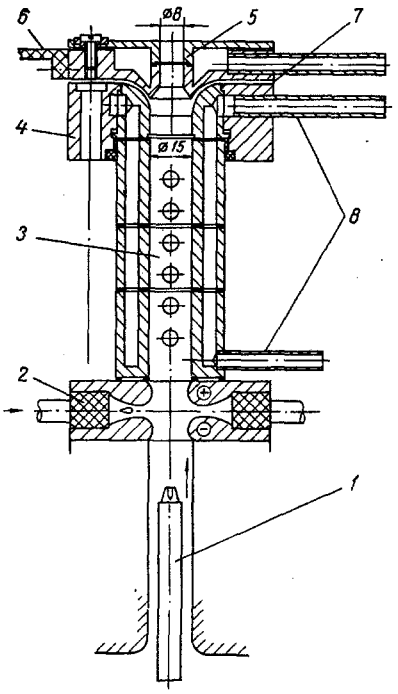

Fig. 1. Cross section of a plasmatron of the 100 V type with an anode unit of special construction: 1) cathode; 2) insulation of auxiliary electrodes; 3) discharge chamber; 4) intermediate element; 5) movable anode; 6) anode holder; 7) slit for removal of part of the argon; 8) cooling water.

We measured the axial velocity and the maximum temperature at the axis of the free jet near the nozzle cut (at a distance of 3 mm). The velocity v_m was determined from the Bernoulli formula $v_m = (2P_{dm}\rho^{-1})^{1/2}$. The dynamic pressure was measured with a miniature Pitot tube with high-intensity cooling (here it was assumed that the condition $P_{st} = P_{bar}$ holds in the jet). The gas density was found from standard tables for the corresponding measured temperature T_m.

To determined the radial and axial profiles of the dynamic pressure we used an automated measurement and treatment system, which is shown schematically in Fig. 2. Since P_{dm} was measured only at the axis of the free jet (r = 0), we used only the part of the system outlined with heavy lines.

The argon temperature was measured by the method of absolute intensity of continuous emission (continuum). In the case of argon in the temperature range of 8000-15,000°K this emission arises in free–free (bremsstrahlung) and free–bound (recombination emission) transitions of electrons in the fields of singly charged ions (Z = 1). The total spectral emission coefficient, including the contributions of these two processes, will be, according to [11],

$$j_\nu(T) = \frac{\sqrt{2}}{24\sqrt{3}\pi\pi^2\varepsilon_0^3}\,\frac{Z^2e^6}{c^3m^{3/2}}\,\frac{N_iN_e}{(kT)^{1/2}}\,\xi(\nu, T). \qquad (1)$$

The value of the Biberman–Norman coefficient $\xi(\nu, T)$ for argon was taken from Schlüter's paper [12].

The measurements were made on an instrument created on the basis of a plasma photometer of the Karl Zeiss Jena Co. [13] with monochromatization by an interference filter. An optical diagram of the instrument is given in Fig. 3.

In the measurements the objective 1 projects part of the free jet onto the plane of the slit 3. The required enlargement of the image is achieved by varying the distance from the objective to the slit; its illumination can be changed by replacing the objective diaphragm 2. A Hartmann diaphragm 4 is used to isolate from the image the part for which the emission intensity is measured. Radiation passing through the opening in the Hartmann diaphragm and

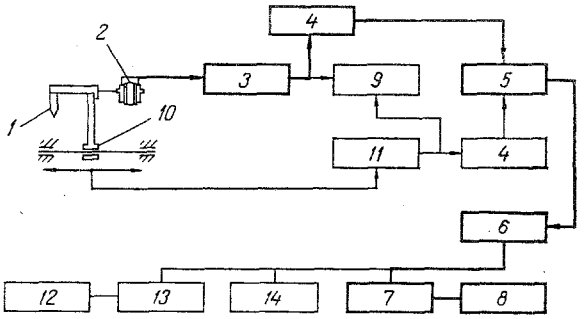

Fig. 2. Schematic diagram of the instrument for automatic pressure measurements and data treatment: 1) Pitot tube; 2) induction pressure sensor of type SE-75; 3) SE-4000 system (source and processing part of the sensor); 4) MT-100 digital voltmeter; 5) EMG-79845 interface of voltmeter; 6) EMG-666 desk-top calculator; 7) typewriter interface; 8) Konsul-260 typewriter; 9) Khanovell recording oscillograph; 10) resistance sensor of probe position; 11) MT-101 resistance-voltage converter; 12) BAK-4T coordinate recorder; 13) EMG-79831 interface of coordinate recorder; 14) EMG-14893 printer.

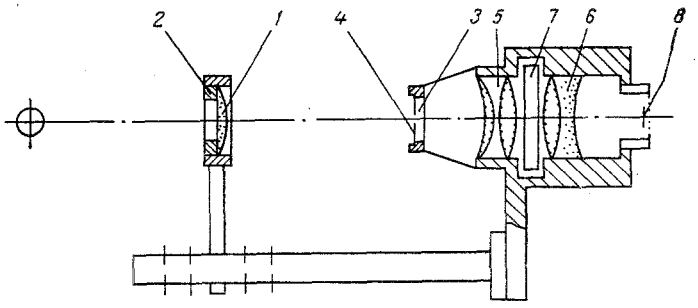

Fig. 3. Diagram of the partial radiometer: 1) objective; 2) interchangeable objective diaphragm; 3) entrance slit; 4) Hartmann diaphragm; 5, 6) two-part condenser; 7) interference filter; 8) photoelement.

the slit enters the interference filter 7 through the first part of the condenser 5. The other part of the condenser 6 focuses the monochromatic radiation onto a selenium photoelement 8, the signal of which is read on a galvanometer scale.

An interference filter with a passband in the region of λ = 630 nm was used in the measurements.

In treating the data we assumed that the measured distribution of emission intensity is nearly axisymmetric and is well approximated by the expression

$$I(y) = I_0 \exp[-(y/r_0)^2]. \tag{2}$$

Under such an assumption, the radial distribution of the emission coefficient will be

$$j(r) = \frac{1}{\pi}\int_0^\infty \frac{\frac{dI(y)}{dy}dy}{\sqrt{y^2 - r^2}} = \frac{I_0}{\sqrt{\pi}\, r_0}\exp[-(r/r_0)^2] = j_0 \exp[-(r/r_0)^2]. \tag{3}$$

The maximum value j_0 and the geometrical parameter r_0 were determined [14] from measurement data on the emission flux from a cross section

$$E = 2\int_0^\infty I(y)\,dy = \sqrt{\pi}\, r_0 I_0 = \pi r_0^2 j_0 \tag{4}$$

and from the maximum intensity

$$I_0 = \sqrt{\pi}\, r_0 j_0. \tag{5}$$

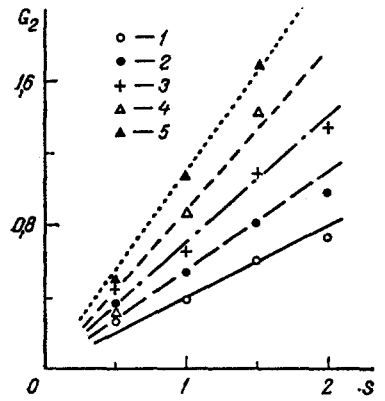

Fig. 4. Amount of removed argon as a function of the slit width (I = 150 A): 1) 1.20 g/sec; 2) 1.68; 3) 2.16; 4) 2.64; 5) 3.12.

The maximum temperature was determined from the value j_0 using Eq. (1). The parameter r_0 is proportional to the radius of the emission core.

3. Experimental Results and Their Analysis

Along with finding the maximum dynamic pressure P_{dm} and the maximum temperature T_m at the axis of a free jet of highly heated argon, we also measured the parameters required to determine the important characteritics of the plasmatron: the power, the efficiency, and the volt–ampere characteristic.

The plasmatron operated in the range of I = 100-175 A and with G = 1.20-3.12 g/sec.

To determine the amount of gas removed through the slit, it would be necessary to use a chamber of more complicated construction with a seal for the movable anode, permitting measurement of the argon flow rate. Since the escaping argon has a temperature of from 350 to 520°K (according to the data of thermocouple measurements), it would also be necessary to cool it. It is simpler, however, to determine the flow rate of removed argon by calculation, using the already established functions for P_{dm}.

To find the maximum dynamic pressure at the axis of the exit nozzle of a plasmatron with an ordinary anode unit we can use the expression

$$P_{dm} = \frac{4536 \cdot 10^{-6}}{D^4} (h_s G^2)^{0,88} \tag{6}$$

or the less precise expression

$$P_{dm} = \frac{0,11\rho + 0,41 \cdot 10^{-3}}{D^4} (h_s G^2)^{4(v_0 \cdot 10^3)^{4,65}}. \tag{7}$$

Equation (6) is valid in the power range up to 0.5 MW; the possibility of using (7) has been shown not only for argon but also for nitrogen and air [15]. To determine the flow rate of removed argon, it is assumed that Eq. (6) is also valid in the case when the mass flow rate of argon through the anode does not equal the flow rate through the discharge chamber. This assumption was confirmed in an investigation of the operation of a plasmatron with gas injection into the discharge chamber in front of the anode [7].

On the basis of this assumption, the mass flow rate G_1 of the argon flowing through the anode can be determined through (6) from the results on the measured pressure P_{dm}. The mass flow rate of argon through the slit is $G_2 = G - G_1$.

The calculations for I = 175 A are represented by the function $G_2 = f(s)$ given in Fig. 4. It is seen from the figure that G_2 varies from 0.23 to 1.7 g/sec (the maximum flow rate G_2 for I = 150 A is 1.8 g/sec, while for I = 100 A it is 1.95 g/sec).

The measured values of P_{dm}, T_m, and r_0 together with certain working characteristics of the plasmatron for a current I = 150 A are given in Table 1. The influence of the removal of part of the working gas ahead of the anode on the electric voltage is similar to the variation in the mass flow rate of gas flowing through the discharge chamber: The value of U decreases

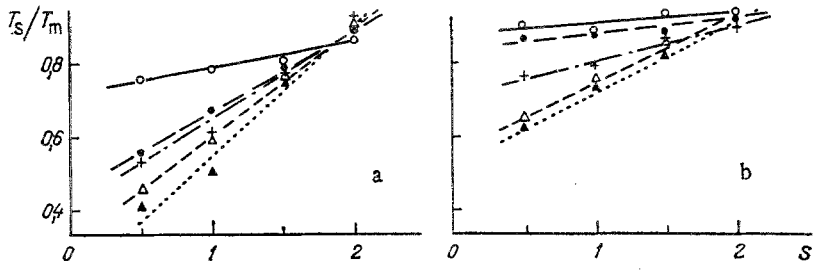

Fig. 5. Ratio T_s/T_m with variation of the slit width (see Fig. 4 for notation): a) I = 100 A, h_s = 2.16-5.5 kJ/g; b) I = 175 A, h_s = 3.92-9.62 kJ/g.

TABLE 1. Measurement Results for a Current Strength of 150 A

Voltage U on electrodes, V	Mass flow rate G, g/sec	Slit width s, mm	Max. dynamic pressure P_{dm}, Pa	Max. temp. T_m, °K	Radius r_0, mm	Efficiency η
82,5	1,20	0,5	4578	11 140	2,07	0,49
82,0		1,0	4287	11 160	2,04	0,48
81,0		1,5	2745	11 080	2,08	0,40
80,5		2,0	1949	11 060	1,99	0,36
87,5	1,68	0,5	7759	11 250	2,07	0,57
87,0		1,0	6954	11 200	2,08	0,55
86,0		1,5	4452	11 190	2,07	0,47
85,0		2,0	3094	11 170	2,10	0,42
92,0	2,16	0,5	10194	11 400	1,90	0,60
91,0		1,0	9505	11 380	1,94	0,58
89,0		1,5	5732	11 360	1,95	0,52
88,0		2,0	3889	11 350	1,95	0,46
94,5	2,64	0,5	13130	11 440	1,82	0,62
93,5		1,0	12034	11 470	1,82	0,61
92,5		1,5	7516	11 450	1,92	0,49
99,9	3,12	0,5	16610	11 490	1,74	0,61
98,0		1,0	14110	11 480	1,85	0,57
96,0		1,5	8651	11 460	1,88	0,52

somewhat with an increase in the slit s. In this case the maximum dynamic pressure decreases considerably, and in some cases P_{dm} reaches only 40% of the value measured for a slit width s = 0.5 mm. The maximum temperatures remain approximately the same. From the table and certain measurements not given in the paper we were able to note a small decrease in T_m with an increase in slit width, but it is within the limits of the measurement error. At higher flow rates one observes a certain increase in the geometrical parameter r_0, proportional to the diameter of the emission core. In the last column of the table we give the thermal efficiency η of the plasmatron, which decreases considerably with an increase in the slit, as can be seen from the table. Similar relations occur for I = 100 and 175 A.

According to some papers, e.g., [16, 17], intense mixing of the cool gas stream near the wall with the hotter gas in the region of the arc occurs in the anode region. Then the measured maximum temperature would have increased because of the removal of some of the cool gas. But T_m hardly increases, judging from the results of our measurements. On this basis, we can conclude that under the experimental conditions the argon flowing through the middle part of the anode in the region of the electric arc does not mix intensively with the cool argon and that the region of the electric arc behaves like an unventilated body to a certain extent. Then as a result of the peeling off of cool argon in the anode region the heat losses increase considerably and the efficiency decreases (see Table 1).

The values of T_s/T_m for I = 100 and 175 A are shown in Fig. 5. It is seen from the graph that for a narrow slit s the temperature profile has an especially steeply sloping character for low currents (100 A) and high argon flow rates and hence low average specific enthalpies of the heated argon stream (h = 2.16 J/g corresponds to G = 3.12 g/ssec). The temperature profile levels out with an increase in the slit in all cases. For a slit width s = 2 mm and a current of 100 A, $T_s/T_m \approx 0.9$ for all G; for a current of 175 A it approaches one.

The situation is somewhat different for the velocity profile, or more precisely, for the ratio v_s/v_m characterizing it. For a constant slit width (e.g., s = 0.5 mm) the profile

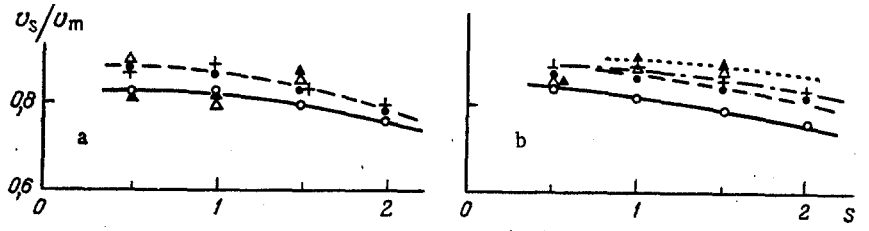

Fig. 6. Ratio v_s/v_m with variation of the slit width (see Fig. 4 for notation): a) I = 150 A, h_s = 3.83-9.74 kJ/g; b) I = 175 A, h_s = 3.92-9.62 kJ/g.

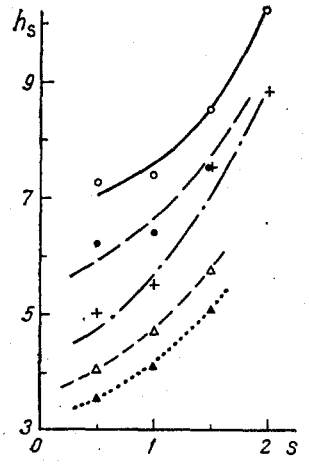

Fig. 7. Variation of enthalpy as a function of slit width (see Fig. 4 for notation).

has a more level character for small G; an increase in s leads to a decrease in the ratio v_s/v_m by a maximum of 10%, and the value of v_m decreases by 50% from the value for s = 0.5 mm with an increase in the slit width s (see Fig. 6).

For comparison we also give the variation of v_s/v_m for a plasmatron operating on argon without gas removal [18]; a) for tangential supply of argon to the discharge chamber

$$\frac{v_s}{v_m} = \frac{0{,}3686}{D^{0{,}23}}\left(1 - \frac{0{,}301}{\log h + 0{,}301}\right); \tag{8}$$

b) for axial flow of argon through the discharge chamber

$$\frac{v_s}{v_m} = \frac{0{,}3686}{D^{0{,}23}}\left(1 - \frac{0{,}204}{\log h + 0{,}204}\right). \tag{9}$$

The functions (8) and (9) were tested for anode opening diameters of from 5.6 to 11.3 mm.

To calculate the ratio h_s/h_m for plasmatrons without gas removal from the discharge chamber one can use [19].

Removal of part of the argon ahead of the anode will also be manifested in an increase in the average enthalpy h_s. As the results of measurements for I = 150 A show (Fig. 7), in certain cases the average enthalpy increases almost twofold. According to [20], for argon the flux density of the heat transferred to an uncooled surface 8 mm in diameter can be determined (under the experimental conditions described in this paper) from the formula

$$q = 9{,}15 \cdot 10^4 \frac{Gh_s}{\mathrm{Re}_m^{0{,}7}}. \tag{10}$$

From this it follows that by removing part of the cool gas from the discharge chamber one can increase the heat flux supplied to the working surface (in plasma sputtering, for example).

4. Conclusion

An analysis of the results of our measurements shows that removal of the cool part of the working gas from the discharge chamber of a plasmatron has slight influence on the maximum

temperature near the nozzle. This indicates that under the given conditions the electric arc in the anode behaves like an unventilated body to a certain extent, while the hot gas mixes insignificantly with the cool boundary stream. An increase in the fraction of removed gas makes the radial temperature distribution more level. This appears particularly for low values of the electric current (where the profile slopes considerably for large flow rates). An increase in G_2 causes a strong decrease in the maximum dynamic pressure and the maximum exit velocity and a considerable increase in the average specific enthalpy of the jet of highly heated argon.

NOTATION

s, width of anode slit, mm; v_m, maximum gas velocity, m/sec; P_{dm}, maximum dynamic pressure, Pa; ρ, gas density, kg/m^3; P_{st}, static pressure, Pa; T_m, maximum temperature, °K; j_ν, $j(r)$, spectral emission coefficient, J/(m^3·sr); ε_0, permittivity, c^2/(J·m); c, speed of light in a vacuum, m/sec; e, electron charge, C; m, electron mass, kg; k, Boltzmann constant, J/°K; Z, multiplicity of ions; N_i, ion concentration, m^{-3}; N_e, electron density, m^{-3}; $\xi(\nu, T)$, Biberman–Norman coefficient; ν, frequency, sec^{-1}; λ, wavelength, m, nm; I(y), spectral emission intensity, J/(m^2·sr); r_0, geometrical parameter of the intensity distribution and emission coefficient, m, mm; I, electric current, A; G, total mass flow rate of the gas, g/sec; G_1, mass flow rate of gas through the anode, g/sec; G_2, mass flow rate of gas through the slit, g/sec; h_s, average enthalpy, kJ/g; D, anode diameter, mm; ν_0, kinematic viscosity in Eq. (7) for T = const = 3000°K, m^2/sec; η, efficiency; U, electric voltage, V: T_s, average temperature, °K; v_s, average velocity, m/sec.

LITERATURE CITED

1. R. Quellette, M. Barbier, and P. Heremisinoff, Technological Application of Low-Temperature Plasma [Russian translation], Moscow (1983).
2. V. Dembovsky, Plazmová Metalurgie, Prague (1978).
3. L. S. Polak (ed.), Plasmachemical Reactions and Processes [in Russian], Moscow (1977).
4. J. Dundr, V. V. Chuprasov, and F. B. Yurevich, Strojnícky Časopis, 33, No. 5, 601-616 (1982).
5. J. Dundr and F. Plojhar, "Hydrodynamická struktura výbojových komor plasmatronú a volného proudu plazmatu a jejich vzájemná souvislost," Správa ÚT ČSAV, Z-791 (1982).
6. J. Dundr and F. Plojhar, "Tlaková a rychlostní struktura volného proudu vysoceohřátého dusíku," Zpráva ÚT ČSAV, Z-913 (1984).
7. J. Dundr et al., "Vliv hydrodynamické kontrakce na strukturu volného proudu vysoceohřátého N_2," Zpráva ÚT ČSAV, Z-866 (1983).
8. J. Dundr and F. Plojhar, IUTAM Symposium on High Temperature Gas Dynamics, Prague, 1981. Proceedings, Inst. Thermomech., Czech. Acad. Sci. (1981), pp. 63-70.
9. J. Dundr, "Uzel výstupní elektrody výbojové komory plazmatronu," Czech. inventor's patent No. 218.921.
10. J. Dundr, "Výstupní otvor výbojové komory," Czech. inventor's patent No. 224.425.
11. L. M. Biberman and G. E. Norman, J. Quant. Spectrosc. Radiat. Transfer, 3, 221-245 (1963).
12. D. Schlüter, Z. Phys., 210, 80-91 (1968).
13. K. Schovanec and J. Šlechta, "Výsledky měření teplot argonu na plazmatronu 100 V," Zpráva ÚT ČSAV, Z-491 (1979).
14. J. Šlechta, "Vliv přifukování chaldného plynu na teplotu dusíku ohřátého plazmatronem," Zpráva ÚT ČSAV, Z-837 (1984).
15. J. Dundr et al., "Experimentální výzkum volného proudu vysoceohřátého vzduchu," Zpráva ÚT ČSAV, Z-908 (1984).
16. M. F. Zhukov, Izv. Sib. Otd. Akad. Nauk SSSR, Issue 2, No. 2, 1-14 (1975).
17. M. F. Zhukov, A. S. Koroteev, and V. A. Uryukov, Applied Dynamics of a Thermal Arc [in Russian], Novosibirsk (1975).
18. J. Dundr, "Hydrodynamická struktura turbulentního paprsku plasmatu," Zpráva ÚT ČSAV, Z-534 (1976).
19. J. Dundr, L. Kreichi, V. L. Sergeev, A. S. Strogii, and F. B. Yurevich, Strojnícky Časopis (in press).
20. J. Dundr and Ya. Kuchera, Inzh.-Fiz. Zh., 33, No. 4, 648-655 (1977).